Development of ECRH-based methods for assisted discharge burn-through: experiment and simulation

D. Ricci[1,*], *J* Stober[2], *R.* Dux[2], *L.* Figini[1], *T.* Wauters[3], *E.* Lerche[4], *G.* Granucci[1], the ASDEX Upgrade Team, and Eurofusion WPTE Team

[1]Istituto per la Scienza e Tecnologia dei Plasmi, CNR, Milan, Italy
[2]Max-Planck-Institut fur Plasmaphysik, Garching, Germany
[3]ITER Organization, Building 72/2026, SCOP, SCOD, Science Division
[4]UKAEA Culham Centre for Fusion Energy, Abingdon

Abstract. Electron Cyclotron (EC) waves will be routinely used in future reactors not only for plasma heating and/or non-inductive current drive during the flat top but also to assist the plasma start-up phase in large toka-maks with superconductive coils. In ITER, for example, EC start-up is foreseen since first plasma operation. To limit the level of stray radiation, ECRH can be used after ohmic breakdown, as a robust solution to successfully sustain the plasma burn-through in the presence of pre-filling gas and impurity influx from the wall.

On ASDEX Upgrade (AUG), a series of dedicated experiments have been performed using EC heating (X2) with a controlled Ne impurity injection in the prefill phase, to mimic non-favourable burn-through conditions such as would be expected in a discharge following a disruption event. The time for EC heating onset has been optimised to assist the early burn-through and a scan of the Ne concentration has been performed to find the threshold for successful burn-through conditions for two ECH power levels (0.7 and 1.4 MW). The toroidal magnetic field flexibility has been also documented, with the cold resonance position being shifted up to 13 % in major radius to match the ITER condition. These experiments showed that optimised settings of ECH power (onset and duration of the pulse) have a key role in making feasible the early Ne burn-through (with Ne concentration up to 14% and EC power of 1.4 MW). Successful pulses will be extended to study stationarity and clean up properties.

For an efficient and robust use of such a technique, it is essential to develop appropriate models capable of de-scribing present experiments and of extrapolating (or predicting) to future scenarios. In this work, the predictive 0D model for the burn-though phase BKD0 [1] has been used to reproduce experimental results and estimate the power required for a successful burn-through as a function of the impurity concentration, finding that ECH power of 1.4 MW is required to sustain burn-through with more than 20% of Ne. The scalability of the model has been also tested on TCV [2] and its implication for ITER will be discussed.

1 Introduction

In the past, several experimental studies have been performed to define the operation scenario especially in view of ITER Electron Cyclotron (EC) assisted start-up. Plasma initiation assisted by EC has been applied successfully on different tokamaks. This method provides additional heating during the pre-ionization of the prefill gas and also during the burn-through, although the influence of EC is different on the two phases [1][3]. On ASDEX Upgrade [3] it was observed that EC heating applied after ohmic breakdown is a valuable way to overcome the radiation barrier, although a systematic study with controlled impurity injection has not yet been performed. In case of ITER, for the burn-through, modelling suggests that the power absorption at the second harmonic of the cyclotron frequency (X2) is not efficient at relatively low temperatures and densities that characterise this phase, both in single-pass scheme foreseen for First Plasma (FP),

as well as in multi-pass configuration [4]. In order to sep-arate the effect and confirm modelling prediction, a series of experiments have been carried out on ASDEX Upgrade in presence of controlled impurity injection. To limit the level of stray radiation, EC operating at X2 has been used after a robust ohmic breakdown to successfully sustain the burn-through of pre-filling deuterium with addition of small amount of Ne. By keeping constant the initial parameters for ohmic breakdown (in terms of toroidal electric field and deuterium density) and varying the Ne content it is possible to mimic non-favourable conditions such as it would be expected in case of impurity influx from the wall. We explore the feasibility of a cleaning discharge by means of EC heating and extrapolate results from various devices to ITER.

---

*e-mail: daria.ricci@istp.cnr.it

2 Experimental set up

In ASDEX Upgrade [5], EC assisted burn-through experiments were performed using X2 heating at 140 GHz with power level at 0.7 and 1.4 MW. The database collected consists of 22 discharges, most of them with toroidal magnetic field B_{tor} on-axis of 2.4 T and radial position of the cold resonance slightly on the high field side, while it was varied from 2.2 to 2.6 T in 4 dedicated discharges to test the field flexibility. Deuterium was injected in the vacuum vessel 100 ms before t = 0 s, together with a controlled Ne puffing, injected at -50 ms. Glow discharge was performed in between discharges to avoid Ne accumulation and get reproducibility. The amount of Ne was comparable to what remains in the machine after a killer gas pulse. Figure 1 shows an overview of typical discharge, here performed with 7% of Ne, B_{tor}: 2.4 T, and EC input power at 1.4 MW. EC wave is injected with a toroidal angle of 3° from equatorial launchers (EL), configuration that typically gives reflection all over the cross section.

Parametric scan in P_{EC} and Ne/D was performed to understand the effectiveness, together with EC timing and toroidal field flexibility, that were additionally explored for optimisation purpose.

In this initial phase of the discharge it is difficult to diagnose the plasma accurately because most of the diagnostics are optimised to measure high n_e and T_e. Moreover, ECE emission is missing, since the level of stray radiation is not compatible with ECE system on AUG. The effect of Ne was analysed using VUV spectroscopy (SPRED) for evidencing Ne penetration into the plasma. Measurement of stray radiation was used to characterise the absorption, which is qualitatively compared with simulation results discussed below.

It is worth to note that Ne burn-through results completed in a time interval between 0.5-1 s, depending on the initial concentration, power level, pulse length etc. In order to characterise the EC effectiveness on the early burn-through, different times are considered for the analysis described in the following sections: T1 = 40 ms (chosen after optimisation discussed below) corresponds to the EC onset after the start of the current rise, that is usually around 30 ms. Because different EC pulse durations were tested, the first 30 ms are considered (T2 = 70 ms) in order to compare results from the entire database. Moreover, at T3 = 90 ms the feedback control on the plasma current starts to run. This time is sufficiently accurate to define criterion for successful Ne burn-through, that is achieved if plasma current reaches 200 kA at T3 (see figure 2).

3 Result and discussion

We choose to characterise the scenario as a function of the concentration of Ne injected before the t = 0 s, calculated by the integral of the corresponding calibrated gas fluxes. A minimum EC pulse duration of 30 ms allows to achieve successful Ne burn-through, at least for an initial concentration below 7%. Figure 2 (right) shows in light blue the developing of the plasma current after 30
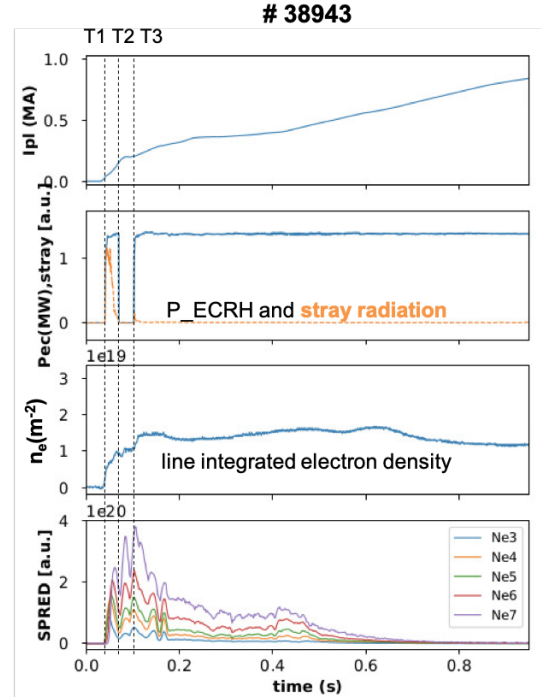
Figure 1. AUG #38943: Overview of EC-X2 assisted burn-through experiment: plasma current, EC power from 40 ms (T1) to 70 ms (T2) and stray radiation, line averaged electron density n_e by interferometry and SPRED signal of NeIII up to NeVII levels. Ne/D: 7%; B_{tor}: 2.4 T
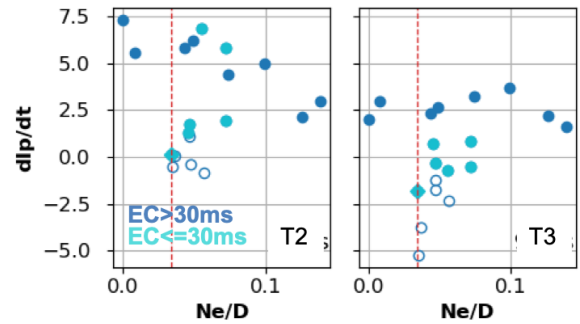
Figure 2. Plasma current development for the present database (B_{tor}: 2.4 T): (left) after the first 30 ms of EC pulse (T2) and (right) when the control of the ohmic coils takes place (T3). Dark blue bullets correspond to successful burn-through for EC blip longer than 30 ms. Light Blue bullets correspond to successful burn-through when EC pulse is up to 30 ms, empty ones to failures. Vertical dashed line is the limit for ohmic case.

ms of ECH power (at T2), giving a clear indications that a longer EC pulse would have helped if compared with the increase at T3 (figure 2, left), burning high level of impurity and making an effective cleaning discharge.

3.1 Optimization

As already outlined in the introduction, focus of the experiments is on the understanding the impact of EC on the burn-through phase only. One of the key point in the scenario developing was the definition the EC timing: not too early because of the need to separate the effect from previous pre-ionization phase, characterised here by a robust ohmic breakdown, and not too late, when the current initially raises and before Ne burn-through starts, to give the wave time to be absorbed in low n_e and T_e conditions.

Two different EC onsets were tested (at 40 and 60 ms, with discharge parameters reported in table 1) aiming to limit the stray radiation level, and making the additional heating effective with and without Ne (see figure 3). Discharge

Table 1. Discharge parameters used to optimise the EC onset

#	$P_{EC}(MW)$	$t_{EC,on}(ms)$	Ne(%)
37949	0.75	60	0
38936	0.75	60	4.7
38940	0.75	40	4.5

without impurity in prefill (figure 3, blue, P_{EC}: 0.7 MW at 60 ms) achieved a sustained burn-through, as expected and reported for comparison. At ECH power of 0.7 MW and Ne 4.5%, the successful case (figure 3, green) is when EC starts at 40 ms instead of 60 ms, which fails. However, the plasma current does not exceed 100 kA, an indication that higher current values could be achieved by increasing the power. The radiation from SPRED (figure 3, bottom panel) reveals that, in this experimental condition, the power is sufficient to create higher level of ionisation up to NeVII, from 55 ms, when absorption starts to improve, as seen from stray radiation signal.

The B_{tor} flexibility was also documented, varying the cold resonance position up to 13% in major radius to match the ITER First Plasma condition [6]. Figure 4 (top) shows the position of the current center R_{curr} and the time evolution of stray radiation up to T3 (bottom). The discharges were performed under identical experimental conditions (prefill, ECH power, Ne/D), except for the B_{tor} on axis, that has been varied from 2.2 T up to 2.6 T. On AUG, current forms close to the inner heat shield, and poloidal field currents are programmed to be identical for all the B_{tor} scan. The radial position of the cold resonances at different fields are indicated by horizontal lines. The EC power level was 1.4 MW. The stray radiation increase significantly in all cases during the first 20 ms of EC pulse. Then it drops for 2.3 T, 2.4 T and 2.6 T in the next 10 ms, leading to sustained burn-through. The 2.2 T case failed, the stray radiation level remains high and tends to move inwards. Heating is more or less in the center of the current, as soon as variation of resonance location R_{EC} is within 10%. Scanning B_{tor} is different from other factors such as ECH power and Ne concentration. It affects the deposition location of ECH power, also with the poloidal magnetic field around it. Many variables make it difficult to analyse the toroidal-field-dependence of the burn-through conditions and give a strong conclusion. The best (rather than optimised) toroidal field should be determined with
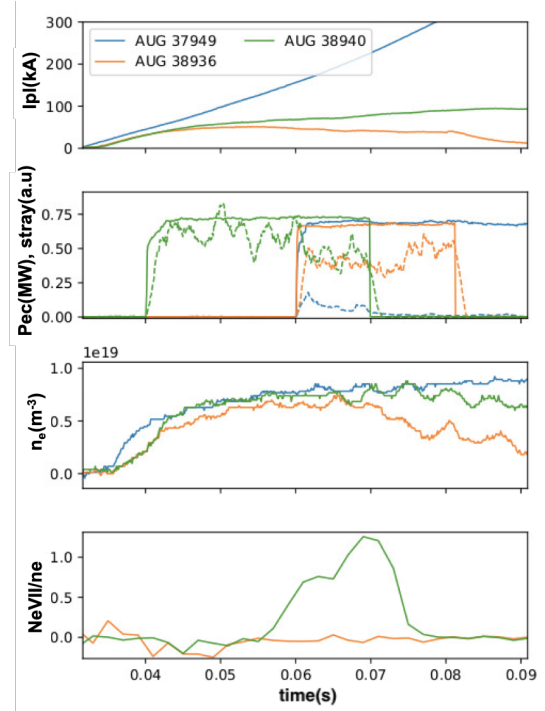

Figure 3. Effect EC onset at 40 or 60 ms, in conditions summarised in Table1. The stray radiation signals are plotted in arbitrary unity. High stray level in #38936 (and consequently low EC absorption) between 60 and 90 ms does not indicate that longer pulse would have helped.

a specific poloidal field (not a fixed poloidal field for all shots). This would require much more detailed experimental scans, which have not been performed yet.
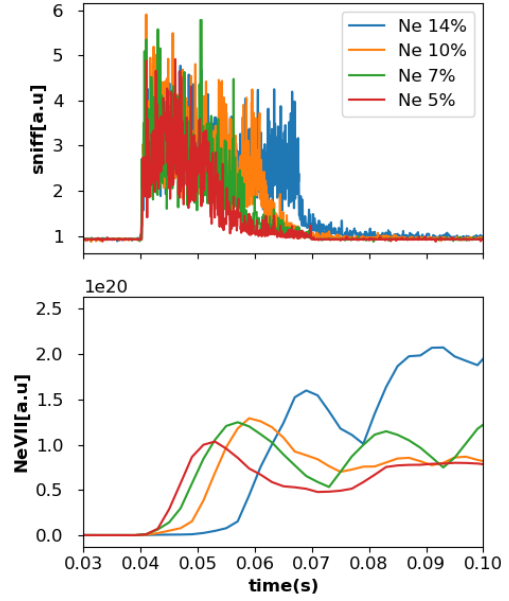
3.2 Ne burn-through

Ne level was measured by SPRED following lines up to NeVII (77.4 nm). As the Ne concentration increases, the integral of NeVII line-emission from SPRED between T1 and T2 decreases (Figure 5), as the derivative of the plasma current does, as already shown in Figure 2(left). This results in keeping the temperature low and making the burn-through of NeVII ion to start with increasing delay. Here different colours correspond to different EC input power: in red no EC power (ohmic); in blue P_{EC}: 0.7 MW; in orange P_{EC}: 1.4 MW. Only few pulses at 0.7 MW are collected due to difficulty in controlling the valve aperture for this rather low Ne flux. Different power thresholds have been identified to achieve sustained burn-through: ohmic heating is sufficient when the Ne concentration is up to 3.5%, P_{EC} = 0.7 MW are necessary to sustain burn-through when Ne is < 4.7% and 1.4 MW makes discharge with Ne impurity up to 14% effective.
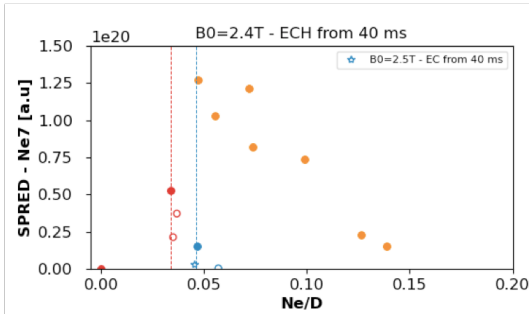
Figure 6 shows the temporal evolution of the 1.4 MW stray radiation of EC for different Ne/D values. As the Ne concentration increases, the stray radiation measured by the sniffer probes also increases due to the low temperature and the delay in NeVII emission line is evident.
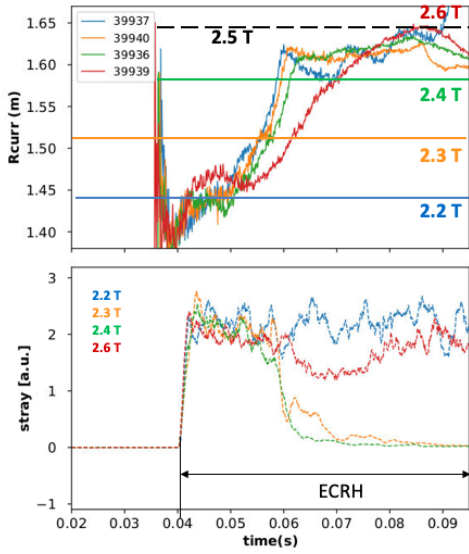
Figure 4. Variation of B_{tor} in the range 2.2-2.6 T, ECH power 1.4 MW, Ne/D= 7%. Top: Position of the current center during EC pulse. Horizontal lines correspond to radial position of cold resonance at corresponding fields. Bottom: stray radiation measurements


Figure 5. As the Ne/D increases, the integral of NeVII calculated from SPRED in the range 40-70 ms decreases. Power thresholds are (red) Ohmic: Ne < 3.5%, (Blue) EC 0.7 MW: Ne < 4.7%, (Orange) EC 1.4 MW: Ne up to 14%. Hollow circles correspond to failure.

To estimate T_e, unavailable from direct measurements at this early stage of the discharge, linear theory of absorption was applied: since sniffer probes exhibit similar temporal behaviour, their signals were used to interpolate between zero and full single pass absorption, which, for X2, scales linearly as the electron pressure as long as the n_e is far below cut-off. The absorption, from the upper panel in figure 7, remains below 30% for the first 10-25 ms of the EC pulse, depending on the Ne concentration, and then rise up. The line integrated n_e was used to determine the T_e (Figure 7 (bottom panel)). This can be considered an upper limit for T_e since a flat n_e profile has been assumed. A peaked n_e profile corresponding to the local electron pressure at the cold resonance location, would reduce T_e.

Considering that the NeVI ion stage lives in the range

Figure 6. Top: Stray radiation increases with increasing Ne/D. Bottom: the derivative of the plasma current decreases (keeping the temperature low) and the burn-through of NeVii line starts with increasing delay. B_{tor}: 2.4 T; P_{EC}: 1.4 MW.

of 0.01-0.4 keV (emission peaks at 31 eV), while NeVII ion stage lives in temperature range 0.02-1keV (emission peaks at 42 eV) (from STRAHL [7], courtesy of M. Cavedon), the central temperature is in good agreement with estimation above.
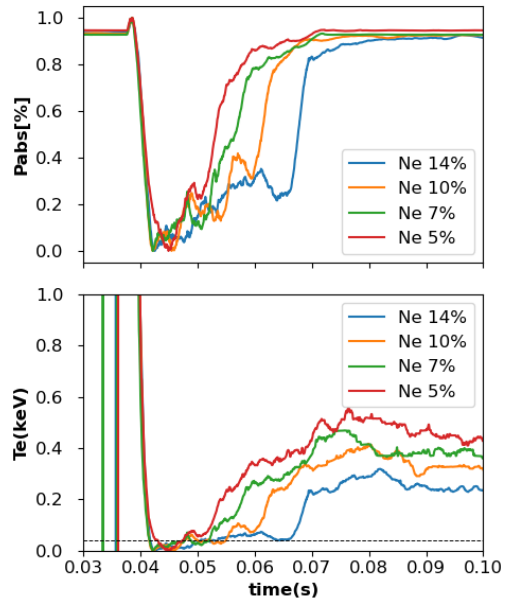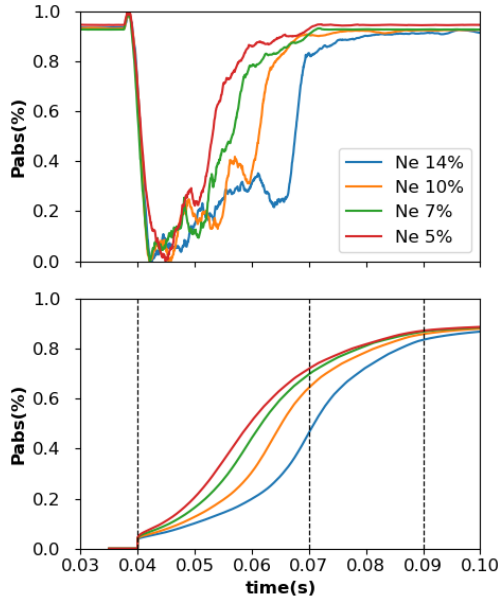

Figure 7. Top: Absorption calculated interpolating non calibrated sniffer probe signals between 0 (no absorption) and 1 (full single pass absorption). Bottom: T_e derived using line integrated n_e and assuming flat density profile.

4 Simulation

To address the question of how much heating power is needed to recover the discharge and assist the Ne burn-through, simulations were carried out with the code BKD0 [1]-[3] to reproduce the experimental data. The model is based on a two-step analysis: a 0D simulation of time evolution of main plasma parameters which contains energy balance equations for electrons and ions, particle balance equations for all the species involved in the simulations (electrons, ions and neutrals as D2 and impurities) and electric circuit equation. This is coupled with the self-consistent calculation of the ECH power absorption done with code GRAY[9]. Figure 8 shows similar trend between measurement and simulation of absorption done with BKD0, and absorbed power calculated by GRAY. The absorption will be discussed below.

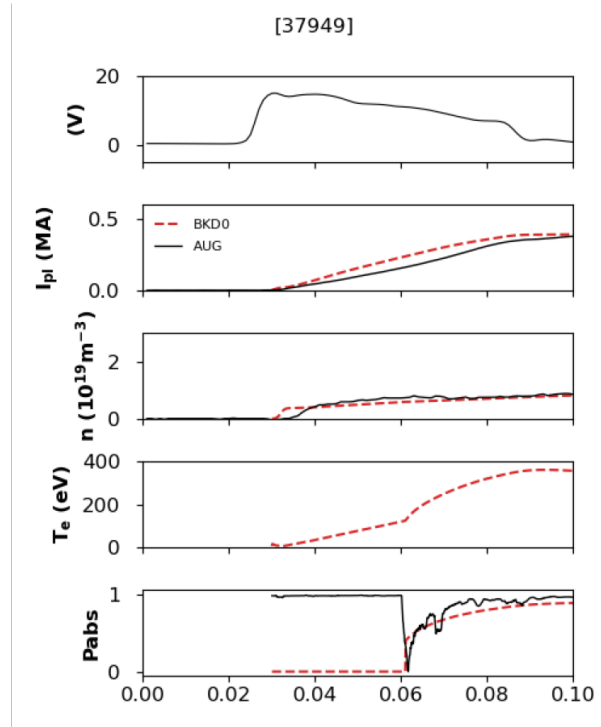An example of simulation is shown in figure 9, based on #37949. The loop voltage measured is used as input. The initial neutral density is derived from in-vessel pressure measurement by midplane gauge at t=0. The n_e is measured by interferometry. The simulated volume-averaged n_e approaches similar values with interferometry data, showing reasonable evolution. The time evolution of the main plasma quantities at different Ne/D and ECH power has been carried out. The effect of Ne was compared with simulation results with the following procedure: for each simulation, given the density of the charged stages of Ne, n_e and T_e, a synthetic diagnostic has been set up. The photon emissivity coefficients (pec), obtained from OPEN-ADAS database [8] were used to perform the interpolation of the data onto the n_e, T_e of the model and calculate the local emissivity via:

$$eps = \frac{1}{4\pi}(pec_{exc}n_e n_z + pec_{rec}n_e n_{z+1}). \qquad (1)$$

Here, eps is the emissivity in $[photons/m^3/s/sr]$, pec_{exc} is the photon emissivity coefficient for excitation and pec_{rec} is the photon emissivity coefficient for recombination $[m^3/s]$.

Finally, integrating eps over the path length of the SPRED (or multiply by 1m because there is no profiles) and adding up all the lines of one-charge stage, SPRED data have been compared with the synthetic diagnostic. Results have been summarised in figure 10 where simulations reproduce quite successfully the experimental results, finding the power threshold for successful burn-through condition and predicting more than 20% of Ne to be injected with 1.4 MW of power. The baseline version of

Figure 8. Comparison between absorption derived by sniffer probe signals using the procedure described in section 3.2 (Top) and the absorption done with BKD0 and GRAY codes (Bottom)

Figure 9. Comparison between BKD0 simulation (dashed red) and experimental time traces (black line) of #37949: Loop voltage, plasma current, volume-averaged n_e, T_e and absorption. P_{EC}: 0.7 MW, $t_{EC,ON}$: 60 ms, neutral pressure: 4mPa, no impurity

the GRAY code, already available in the ITER Integrated Modelling & Analysis Suite (IMAS), models the EC beam propagation, absorption and current drive for a single pass of the beam into the plasma. This approach is adequate for modelling scenarios with strong EC absorption, in which the plasma is optically thick and the beam is fully absorbed before reaching the central column of the tokamak, but a description of the beam propagation and absorption after its reflection off the inner wall is necessary for a more accurate modelling of the break-down and burn-through phases, when single-pass EC absorption is still low. A simple model for the
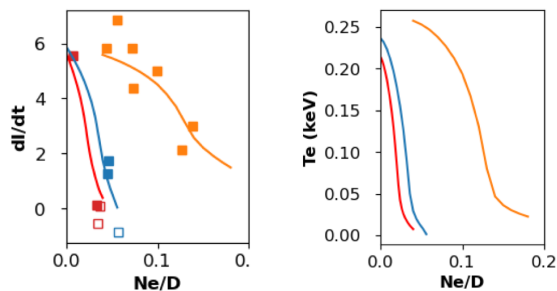
Figure 10. After 90 ms of simulation, red: Ohmic; Blue: EC: 0.7 MW; Orange: EC 1.4 MW. (Left) Comparison between plasma current development as a function of Ne concentration: experimental data (squares), simulation (line). (Right) simulation of T_e as a function of Ne.

reflection of the EC beam on the first wall was included in GRAY, and it has now been implemented in IMAS. The inclusion of the wave reflection model required a change to the code interface: the first wall shape is now needed as additional input in order to compute the geometry of the beam reflection. The reflection model assumes a loss-less ideal conductor with a smooth surface at the wall, so that the full power of the incident beam is transferred to the reflected one, and the reflection is described by Snell's law. Given the assumption that only n_e, T_e close to the EC resonance affects the EC absorption calculation (absorption is localised within few mm from the EC resonance and the exact shape of the null and of the kinetic profiles is not relevant), the shape of the plasma in the poloidal field null region has been simplified to a circular poloidal cross-section where the major radius and the minor radius are Rsim=1.65 m and asim=0.5 m, respectively. This region is crossed both by the injected and by the reflected beam, in conditions where B_{pol}/B_{tor}<1%.

5 Conclusion and outlook

In the case of ITER First Plasma, burn-through modelling suggests that, at the second harmonic, power absorption is limited even in multi-pass configuration. A series of experiments were designed and performed on ASDEX Upgrade, aimed at answering the clear research question related to the EC absorption during this initial phase of the discharge, and confirm prediction. We chose to separate the EC heating effect on pre-ionization phase, starting with a robust ohmic breakdown and a controlled Ne impurity injection in the prefill phase, and started the heating soon after the current rise. We found that key parameters that strongly affect early impurity burn-through are onset

and duration of EC pulse, that needs to be optimised. Furthermore, variations of more than 10% of the cold resonance position need be explored by modification of poloidal field coils currents, optimising the shape of the magnetic configuration. We found the ECH power thresholds as a function of Ne concentration, and the simulations reproduced quite successfully experimental outputs experimental results. Furthermore, sniffer probe signals show that absorption is below 30% for the first 20-25 ms of the EC pulse, and the same behaviour was reproduced by BKD0 and GRAY simulations.

Direct comparison with previous experiments carried out on TCV is not possible due to the different conditions explored: low loop voltage, which means the need to also assist pre-ionization phase by EC, and ECH power actively controlled to keep constant the derivative of the plasma current.

However, the model was applied to TCV (R/a: 0.88/0.25 m) to test scalability. Preliminary simulations show that 0.7 MW of power (82 GHz, X2) is capable of sustaining burn-through of half the concentration of impurities, but must be verified with further dedicated experiments. Open questions that play an important role and will have implication for ITER are related with pre-fill pressure, level of impurities released in the plasma in case of high stray radiation level and wall recycling.

References

[1] G. Granucci, *et al.*, Nucl. Fusion **55** 093025 (2015)

[2] D. Ricci *et al.*, Proc. of the 46rd EPS Conf. on Plasma Physics O5-103 (2019)

[3] J. Stober *et al.*, Nucl. Fusion **51** 083031 (2011)

[4] D. Ricci *et al.* Proc. of the 43rd EPS conference on Plasma Physics O5.130 (2016)

[5] J. Stober *et al.*, Plasma Phys. Control. Fusion 62 024012 (2020)

[6] ITER Research Plan, ITER Technical Report ITR-18-003

[7] R. Dux,STRAHL user Manual, Preprint IPP (2006)

[8] https://open.adas.ac.uk

[9] D. Farina, Fusion Sci. Technol.**52**, 154 (2007)